

Gravity Field And Interior Structure Of Rhea

John D. Anderson^a, Nicole J. Rappaport^a,
Giacomo Giampieri^b, Gerald Schubert^c, William B. Moore^c

^a*Jet Propulsion Laboratory, California Institute of Technology
Pasadena, California 91109-8099*

^b*Space and Atmospheric Physics, Imperial College
London SW7 2BW, UK*

^c*Department of Earth and Space Sciences
Institute of Geophysics and Planetary Physics
University of California Los Angeles, California 90095-1567*

Abstract

Doppler data generated with the Cassini spacecraft's radio carrier waves at X and Ka band can be used to determine the quadrupole moments of Rhea's gravitational field. The resulting tri-axial field should be consistent with the assumption that Rhea is in tidal and rotational equilibrium. If so, we can construct interior models that are consistent with Rhea's mean density of 1236 kg/m^3 , determined previously from Pioneer and Voyager data, and its axial moment of inertia, to be determined from Cassini's gravity data. Two-zone models consisting of a rocky core overlaid by a deep layer of ice are explored in some detail. While three-zone models consisting of an iron core, or a eutectic mixture of iron and iron sulfide, plus a rocky mantle and an outer layer of ice are possible, Rhea's relatively small density suggests that the satellite is not iron rich. Finally, we show that a flyby at the planned altitude of 500 km provides sufficient accuracy for the gravity experiment.

Key words:

Email addresses: John.D.Anderson@jpl.nasa.gov (John D. Anderson),
Nicole.J.Rappaport@jpl.nasa.gov (Nicole J. Rappaport),
g.giampieri@ic.ac.uk (Giacomo Giampieri), schubert@ucla.edu (Gerald
Schubert), bmoore@avalon.ess.ucla.edu (William B. Moore).

ence in the equatorial moments of inertia by

$$C_{22} = \frac{B - A}{4MR^2} \quad (2)$$

where the ellipsoidal satellite's principal moments of inertia are A, B, and C ($C > B > A$). The satellite's total mass is M and its mean radius is R. For a body in rotational and tidal equilibrium¹, the gravity coefficient C_{22} is related to the rotational response parameter q_r by

$$C_{22} = \frac{1}{4}k_f q_r \quad (3)$$

where k_f depends on the distribution of mass within the satellite ($k_f = 3/2$ for constant density). The other principal quadrupole gravity coefficient J_2 is just $10/3$ of C_{22} for a synchronously rotating satellite.

Given C_{22} or J_2 , and q_r , we can determine k_f from Eqn. (3), and the satellite's axial moment of inertia C follows from the Radau relationship (5)

$$\frac{C}{MR^2} = \frac{2}{3} \left[1 - \frac{2}{5} \left(\frac{4 - k_f}{1 + k_f} \right)^{1/2} \right] \quad (4)$$

3 Rhea Interior Models

Consistent with the constraint provided by the single density datum $\bar{\rho}$, we assume a simple two-layer model for Rhea consisting of a core of radius r_c and density ρ_c surrounded by a mantle of density ρ_m . The mean density $\bar{\rho}$ for this two-layer model is

$$\bar{\rho} = \left(\frac{r_c}{R} \right)^3 (\rho_c - \rho_m) + \rho_m \quad (5)$$

Even for this simple model, there is only one equation in three unknowns. Therefore, assume that Rhea's core is made up of material similar to Io's mantle with a density ρ_c of 3250 kg/m^3 (6) and an icy shell of density 1000 kg/m^3 . Eq. 5 yields a fractional core radius $r_c/R = 0.472$. This is certainly a reasonable model, even though the assumption on core density is questionable.

¹ This assumption of equilibrium means that the potential of degree two is determined by the body's response to the rotational and tidal stresses.

where, as illustrated in Fig. 4, b is the spacecraft's distance from the body's baricenter, v is its velocity (all quantities refer to the closest approach time $t = 0$), ℓ and m are the direction cosines for the Earth-spacecraft direction projected, respectively, along the radius and velocity vectors at closest approach, and $r(t) = \sqrt{b^2 + v^2 t^2}$ is the modulus of the (unperturbed) radius vector (7).

In order to construct the covariance matrix we need the partial derivatives of the observable q with respect to the parameters, in our case:

$$\mu \frac{dq}{d\mu} = -m + \frac{mb}{r(t)} - \frac{\ell vt}{r(t)} \quad (8)$$

$$b \frac{dq}{db} = m \left[1 - \left(\frac{b}{r(t)} \right)^3 \right] + \frac{2\ell vb^2 t}{r^3(t)} + \ell \left(\frac{vt}{r(t)} \right)^3 \quad (9)$$

In general, the partial derivatives form the row matrix $\underline{A}(t)$, from which the information matrix is derived as

$$\underline{J} = \frac{1}{T} \int_{t_0}^{t_0+T} \underline{A}^T(t) \underline{A}(t) dt \quad (10)$$

where $[t_0, t_0 + T]$ is the observation interval. Finally, the covariance matrix is given by

$$\underline{C} = \underline{J}^{-1} \sigma_q^2 \quad (11)$$

where σ_q is the expected range rate error; at X-band, we adopt $\sigma_q = 0.015$ mm/sec at 60 seconds integration time, which corresponds to a 2-way Doppler frequency shift of $\Delta\nu/\nu = 2.4 \times 10^{-14}$ (see section 5). The integral in eq. (10) is approximated with a discrete sum, with a sampling time of $\Delta t = 60$ sec. Note that eq. (11) gives a conservative estimate of the error, since we are not dividing by the number of data points N as if all the data errors were random. Instead, we are including the worst possible systematic errors, which heuristically provides a realistic estimation for the error for orbit determination problems.

We can now insert the flyby conditions for Rhea. In our notations these are:

$$b = 1264 \text{ km} \quad (12)$$

$$v = 7.27 \text{ km/sec} \quad (13)$$

$$\ell = 0.14 \quad (14)$$

$$m = -0.95 \quad (15)$$

coefficients, along with other parameters in the fitting model, are determined from the Cassini radio Doppler data by weighted least squares (9; 10; 11; 12).

Next, we examine the Rhea targeted flyby in the Cassini tour of the solar system. This flyby occurs on November 26, 2005.

Figure 8 shows the effects of the quadrupole moments of Rhea’s gravity field on the hyperbolic orbital elements of the spacecraft over an interval of time of one hour around closest approach. The definition of the classical hyperbolic elements follows. Consider the “orbit reference frame” whose (i) origin coincides with the hyperbola’s focus; (ii) x-axis direction is that of the hyperbola’s vertex; and (iii) z-axis direction is normal to the plane of the hyperbola. The semi-major axis ($a < 0$) and eccentricity ($e > 1$) define the shape of the orbit in this reference frame in terms of the cylindrical coordinates r (radius) and f (true anomaly) by

$$r = \frac{a(1 - e^2)}{1 + e \cos f}. \quad (17)$$

Furthermore, the longitude of the node Ω , inclination I , and argument of periapsis ω are the Euler angles orienting the orbit reference frame with respect to a body-fixed reference frame.

In Fig. 8, the signal can be seen clearly over a duration of ± 6 minutes or $\sim \pm 2b/v$ seconds around closest approach. This short duration indicates that closest approach tracking data are very important to determine Rhea’s low order and degree gravity field. In order to quantify the capability of the Cassini experiment, we performed numerical covariance analyses.

An important input parameter to such analyses is the Allan deviation. Our Allan deviation budget benefits from published X-band noise statistics (13). The major noise contributors are the Earth’s troposphere, the charged particles in the interplanetary plasma and the Earth’s ionosphere, and ground antenna mechanical vibrations; the contributions of the ground and spacecraft electronics to the noise can be neglected; the spacecraft attitude is maintained by the reaction wheels, so that translational accelerations associated with attitude control are not of concern. Let us consider an integration time of 1000 seconds.

The one-way Allan deviation associated with the uncalibrated tropospheric noise is typically $\sim 10^{-14}$ if the weather is good but can be six times worse in bad weather. We adopt these two limits for the expected and worst cases, respectively.

Around closest approach, an uplink X-band radio signal will be transmitted

similar behavior. This suggests that high correlations can be expected. We decreased the correlations between (μ or ν) and b by tracking the spacecraft not only around closest approach (from -2 hours to $+2$ hours) but also on the “wings” of the flyby, from -8 hours to -6 hours, and from $+6$ hours to $+8$ hours.

The addition of data on the wings also improved the orbit determination. Indeed, it decreased the uncertainties of all variables except for C_{20} and decreased all the correlations, except those involving C_{20} . This is not surprising in view of the fact that the flyby is nearly equatorial (the spacecraft orbital inclination with respect to Rhea is ~ 10 degrees). For this reason, we removed C_{20} from the set of variables to determine, fixing its value to $-10/3$ the value of C_{22} , as predicted by the equilibrium theory. Thus we determined nine variables consisting of the above-mentioned set of X_k minus C_{20} .

The major results of this analysis (nominal case) are: (1) μ is determined with an absolute accuracy of 3.6×10^{-5} , which is less optimistic by a factor four than found in section 4; (2) C_{22} is determined with an absolute accuracy of 1.8×10^{-6} ; (3) The magnitude of \vec{A} is very well determined; this was verified by comparing the nominal case with one in which this variable is not determined; this confirms the capability of our scheme to account for constant unmodeled forces and systematic errors.

A reduced tracking coverage removing ± 12 minutes around closest approach from the above-mentioned nominal coverage was also considered. This option, if compatible with the scientific goal of the Rhea gravity science experiment, would have had the merit of releasing observation time for any of the other eleven groups of instruments onboard the Cassini orbiter. Indeed, the Cassini tour of the Saturnian system has only one targeted flyby of Rhea. Thus, this option was considered because of the potential increase in science return that it might offer. However, we found that the accuracy of C_{22} determination was degraded to 50×10^{-6} , demonstrating that this option is incompatible with our scientific goal.

6 Conclusions

1) The Cassini Rhea gravity science experiment is expected to determine C_{22} with an accuracy of $\sim 2 \times 10^{-6}$, providing a very good experiment. This in turn will allow us to determine the size and density of Rhea’s core to within 16 % in all plausible cases (see Fig. 3).

2) In the best case, C_{22} would be determined with an accuracy of 1×10^{-6} , providing an excellent experiment.

References

- [1] Davies, M.E., and F.R. Katayama 1983. The control network of Rhea. *Icarus* **56**, 603-610.
- [2] Campbell, J.K., and J.D. Anderson 1989. Gravity field of the Saturnian system from Pioneer and Voyager tracking data. *Astron. Jour.* **97**, 1485-1495.
- [3] Cohen, E.R., and B.N. Taylor 1999. The fundamental physical constants. *Phys. Today* **52**, BG5-BG9.
- [4] Anderson, J.D., R.A. Jacobson, T.P. McElrath, W.B. Moore, G. Schubert, and P.C. Thomas 2001. Shape, mean radius, gravity field, and interior structure of Callisto. *Icarus* **153**, 157-161.
- [5] Rappaport, N., B. Bertotti, G. Giampieri, and J.D. Anderson 1997. Doppler measurements of the quadrupole moments of Titan. *Icarus* **126**, 313-323.
- [6] Anderson, J.D., R.A. Jacobson, E.L.Lau, W.B.Moore, and G. Schubert 2002. Io's gravity field and interior structure. *JGR-Planets* **106**, 32,963-32,969.
- [7] Anderson, J.D., and G. Giampieri 1999. Theoretical Description of Spacecraft Flybys by Variation of Parameters. *Icarus* **138**, 309-318.
- [8] Kaula, W. M., *Theory of Satellite Geodesy*, 124 pp., Blaisdell, Waltham, Mass., 1966.
- [9] Moyer, T. D., Mathematical formulation of the double precision orbit determination program (DPODP), *Tech. Rep. No. TR 32-1527*, 160 pp., Jet Propulsion Laboratory, Pasadena, Calif., 1971.
- [10] Tapley, B. D., Statistical orbit determination theory, in *Recent Advances in Dynamical Astronomy*, edited by Tapley, B. D. and V. Szebehely, pp. 396-425, Reidel, Dordrecht, Netherlands, and Boston, Mass., 1973.
- [11] Anderson, J. D., Lectures on physical and technical problems posed by precision radio tracking, in *Experimental Gravitation*, edited by Bertotti, B., pp. 163-199, Academic Press, New York, 1974.
- [12] Lawson, C. L. and R. J. Hanson, *Solving Least Squares Problems*, 340 pp., Prentice-Hall, Englewood Cliffs, N. J., 1974.
- [13] Armstrong, J.W. 1998. Radio wave phase scintillation and precision Doppler tracking. *Radio Science* **33**, 1727-1738.
- [14] Armstrong, J.W., R. Woo, and F.B. Estabrook 1979. Interplanetary Phase Scintillation and the Search for Very Low Frequency Gravitational Radiation. *Ap. J.* **230**, 570-574.
- [15] Rappaport, N.J., G.G. Giampieri, and J.D. Anderson 2001. Perturbations of a Spacecraft Orbit during a Hyperbolic Flyby. *Icarus* **150**, 168-180.

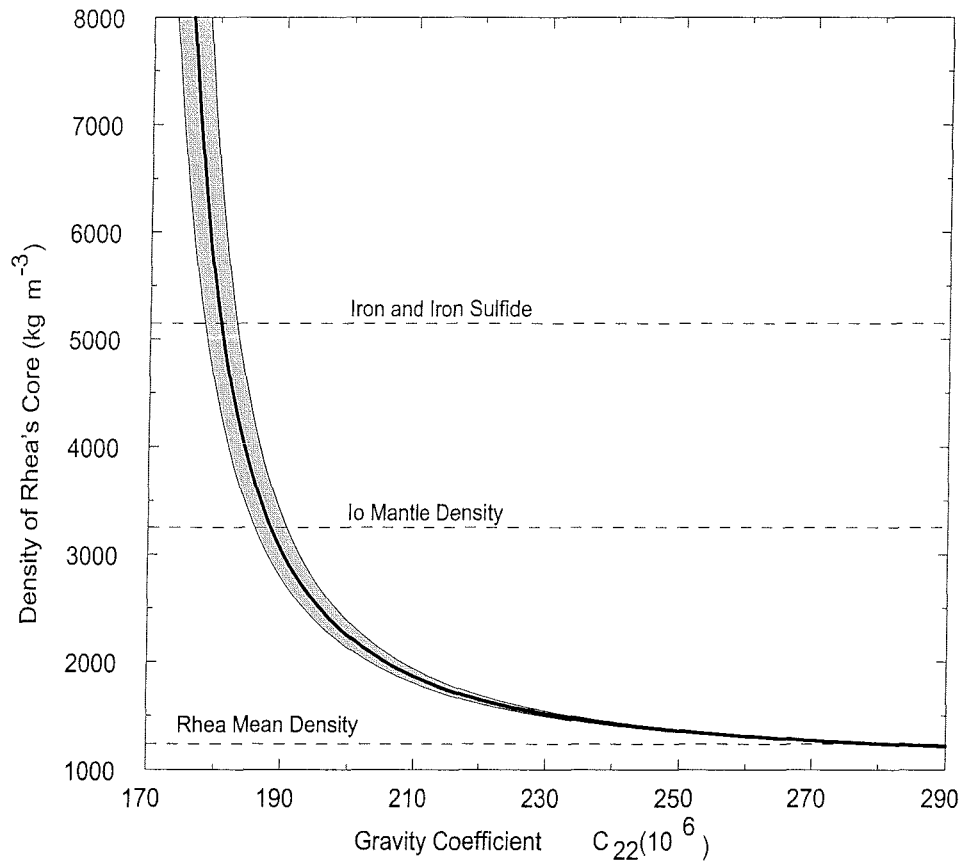


Fig. 1. Rhea's core density as a function of C_{22} . The dashed lines represent Rhea's mean density, the density of Io's mantle as determined from Galileo gravity data, and the density of a eutectic mixture of iron and iron sulfide. The shaded region illustrates how a measurement error of $\pm 2.4 \times 10^{-6}$ is reflected in the density uncertainty.

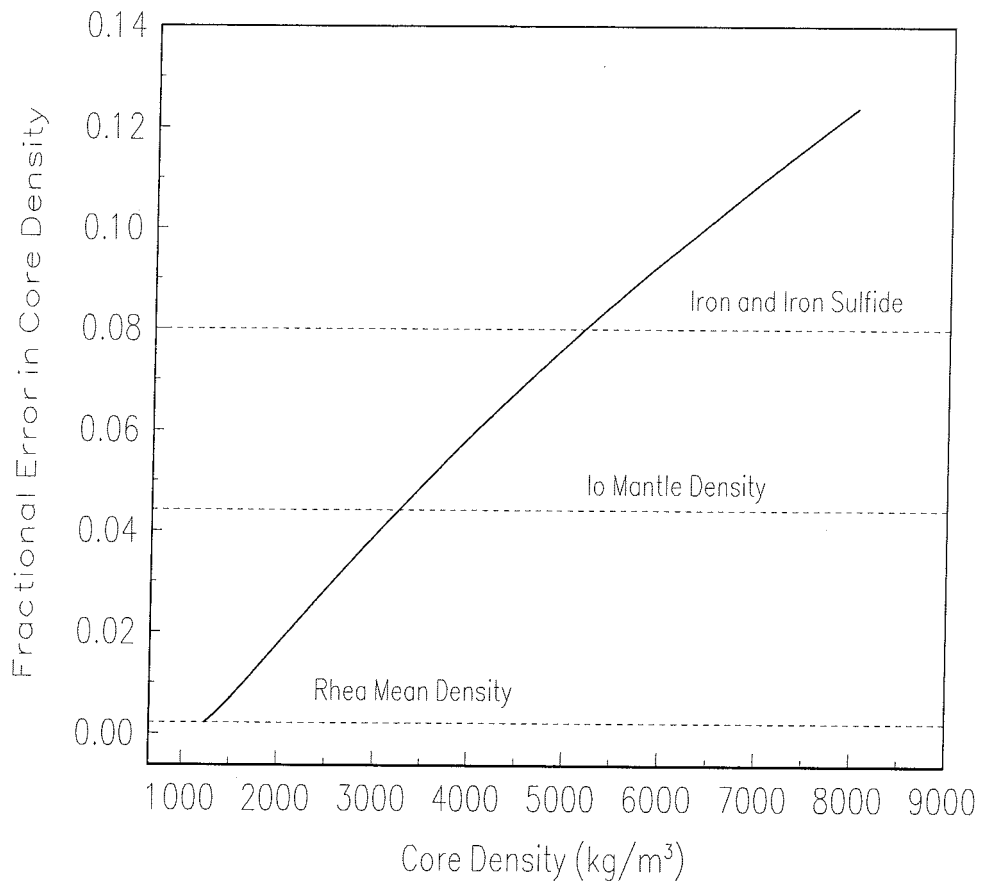


Fig. 3. Fractional error in Rhea's core density as a function of core density for an assumed error of 10^{-6} in the gravity coefficient C_{22} . The dashed lines have the same meaning as in Fig. 1.

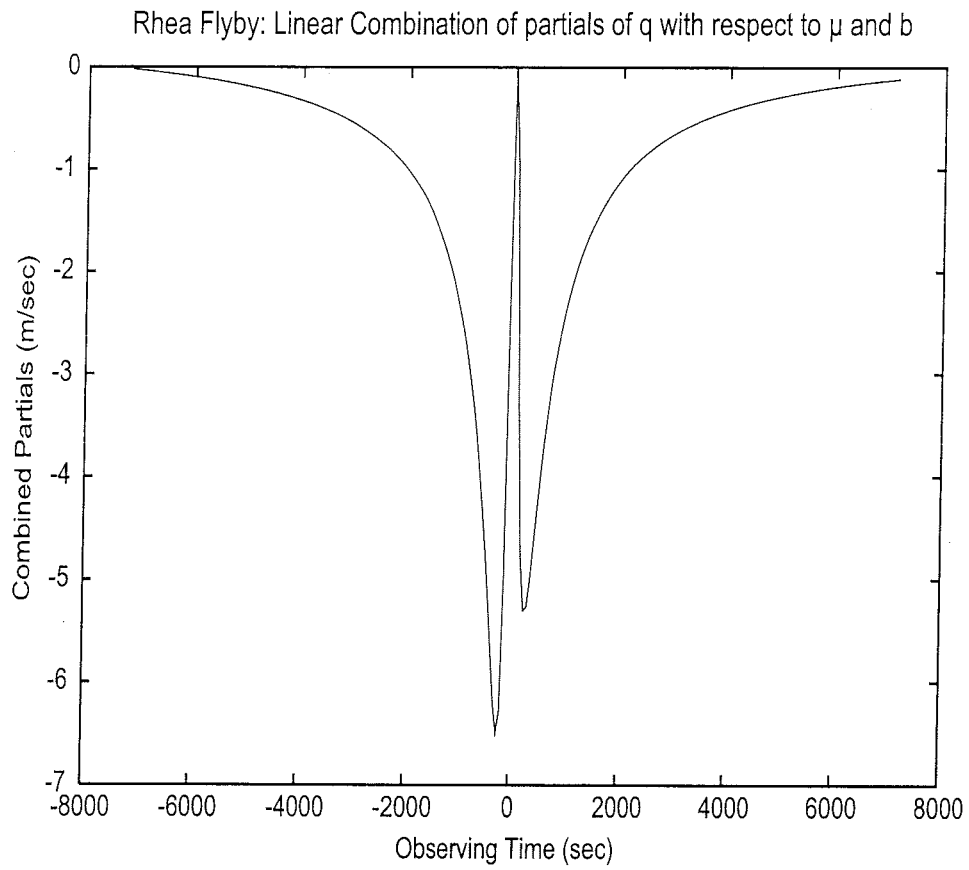


Fig. 5. Linear combination of q partial derivatives with respect to μ and b for Rhea flyby.

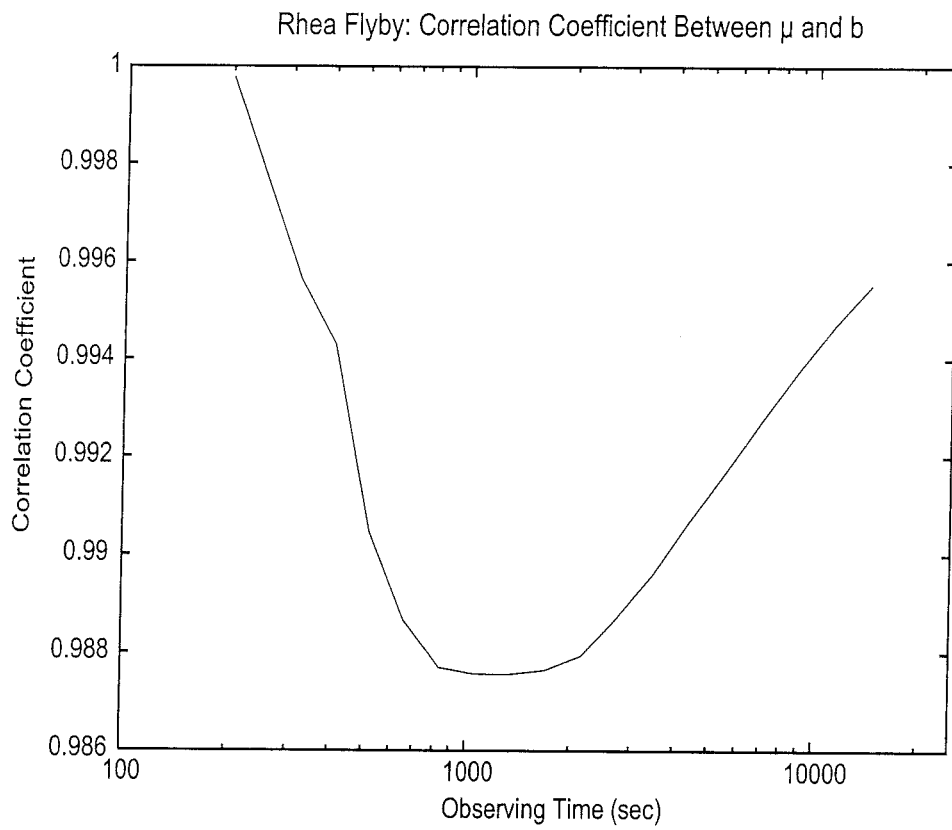


Fig. 7. Predicted correlation coefficient between μ and b for Rhea flyby.

Rhea Targeted Flyby
 Solid line = numerical, circles = analytical

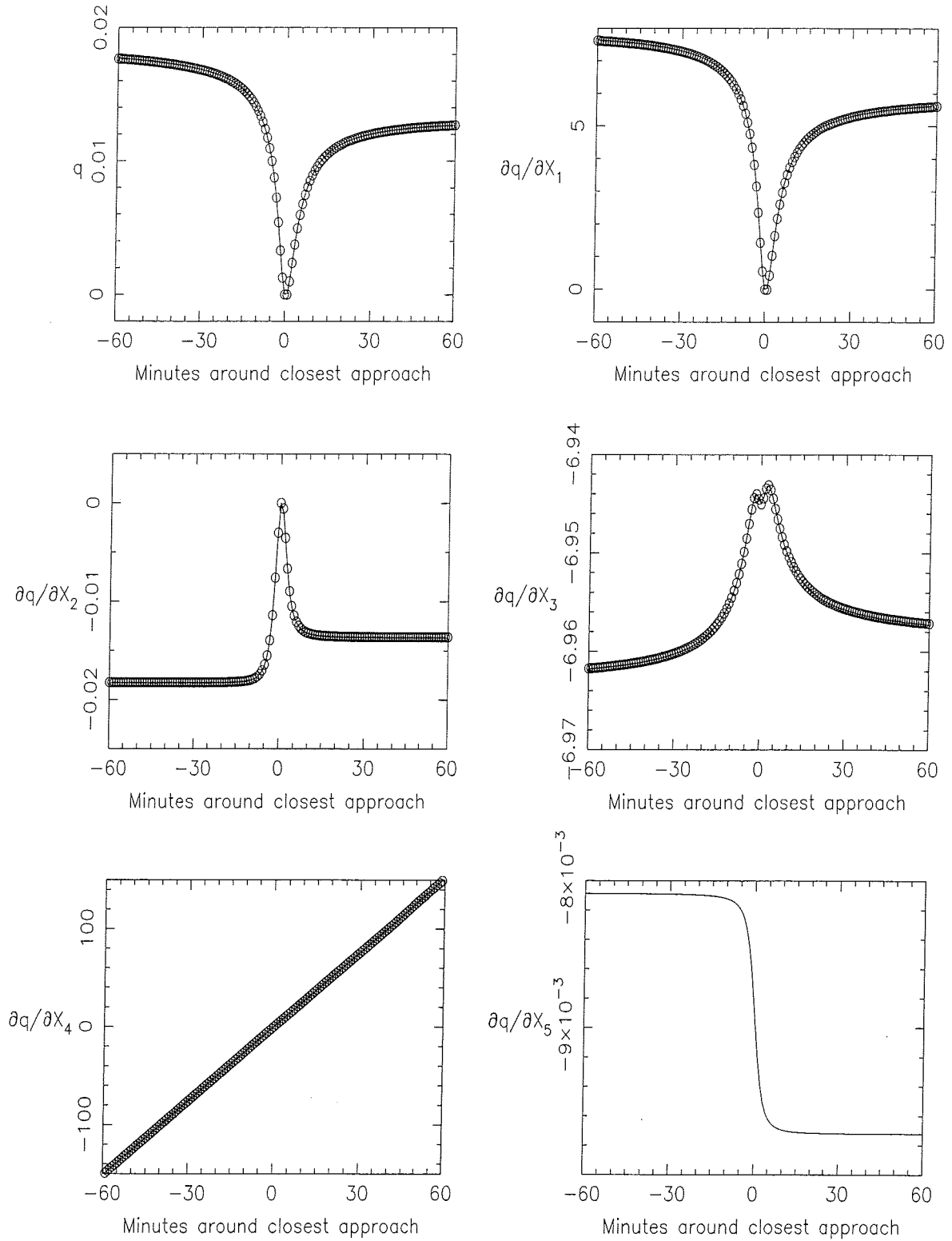


Fig. 9. Doppler observables and partial derivatives of the Doppler observables with respect to the ten fit variables defined in the text. On the vertical scale, the unit is km/s.